DALTON
FULL PAPER

Characterization of two conformers in the co-ordination chemistry of 3,4-bis(cyanamido)cyclobutane-1,2-dione dianion: syntheses, crystal structures, and electrochemical study of nickel(II) complexes

Anne Marie Galibert,[a] Olivier Cortadellas,[a] Brigitte Soula,[a] Bruno Donnadieu[b] and Paul-Louis Fabre*[a]

[a] *Laboratoire de Chimie Inorganique, EA 807, Université Paul Sabatier, 118 route de Narbonne, 31062 Toulouse, Cedex 04, France. E-mail: fabre@chimie.ups-tlse.fr*
[b] *Laboratoire de Chimie de Coordination, UPR CNRS 8241, 205 route de Narbonne, 31077 Toulouse, Cedex 04, France*

Received 27th February 2002, Accepted 23rd July 2002
First published as an Advance Article on the web 4th September 2002

Three complexes $[Ni(Him)_4(3,4\text{-}NCNsq)(H_2O)]\cdot H_2O$ **1**, $\{[Ni_2(Him)_2(3,4\text{-}NCNsq)_2(H_2O)_6]\cdot 8H_2O\}_n$ **2** and $[Ni(tren)(3,4\text{-}NCNsq)]_n$ **3**, where 3,4-$NCNsq^{2-}$ = 3,4-bis(cyanamido)cyclobutane-1,2-dione dianion and Him = imidazole, have been synthesized and characterized by electronic absorption and IR spectroscopies. The structures of the three complexes have been determined by X-ray crystallography and, for the first time, two conformations of the ligand 3,4-$NCNsq^{2-}$ have been evidenced. Complex **1** consists of mononuclear entities and complexes **2** and **3** are made of infinite chains with nickel(II) atoms bridged by the bis monodentate 3,4-$NCNsq^{2-}$ ions. The magnetic properties of the three complexes have been investigated in the 2–300 K temperature range (μ_{eff} = 2.84 to 3.12 μ_B for **1**, μ_{eff} = 2.32 to 3.46 μ_B for **2** and μ_{eff} = 2.74 to 3.13 μ_B for **3**). Their redox properties are discussed and compared to those of the free 3,4-$NCNsq^{2-}$ dianion.

In the course of studies on polymeric co-ordination compounds, complexes of nickel(II) with the squarate dianion $C_4O_4^{2-}$ have been investigated. The magnetic behaviour of the nickel squarate complex $Ni(C_4O_4)(H_2O)_2$ was studied by Gerstein and Habenschuss[1] in 1972 and revealed ferromagnetic interactions at very low temperatures. Two years later, these authors proposed a polymeric structure for this complex on the basis of X-ray powder patterns and magnetic data.[2] The structure consists of layers of squarato-O^1,O^2,O^3,O^4 bridged nickel(II) ions and the octahedral co-ordination of the metal atom is completed by two water molecules in *trans* positions. This structure was confirmed in 1986 by the X-ray resolution of $[Ni(C_4O_4)(H_2O)_2]_3\cdot CH_3CO_2H\cdot H_2O$, a three-dimensional polymer complex.[3] Other structural data reported on squarato nickel(II) complexes have revealed that this particularly interesting ligand may also co-ordinate in a bidentate mode, O^1,O^3- or O^1,O^2-squarato bridged nickel(II) atoms leading to chains or dimeric compounds.[4–7] Nevertheless, magnetic measurements reported on squarato-bridged nickel(II) dimers or chains show that no or only weak antiferromagnetic interactions occur between paramagnetic centres.

New ligands derived from oxocarbons (the $C_nO_n^{2-}$ family) may be obtained by substituting one or more of the oxygen atoms by other atoms or groups (sulfur, selenium, nitrogen, dicyanomethylene, cyanamido,. . .). These pseudo-oxocarbons,[8] characterized by extensive π electrons delocalisation associated with interesting redox behaviour and strong colours (some of them being considered as cyclobutenediylium dyes),[9,10] may present a new challenge in co-ordination chemistry. Herein, our interest is focused on pseudo-oxocarbons containing the cyanamido group NCN, such as 3,4-bis(cyanamido)cyclobutane-1,2-dione dianion derived from the squarate dianion.[11]

An analogy may be pointed out between cyanamido-squarate ligands and 1,4-dicyanamidobenzene dianion ($dicyd^{2-}$), the reduced form of *N*,*N*′-dicyanoquinodiimine (DCNQI).

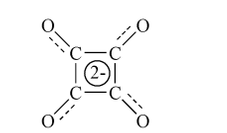

squarate dianion
$C_4O_4^{2-}$ or sq^{2-}

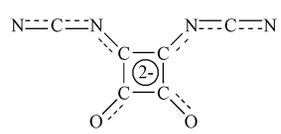

3,4-$NCNsq^{2-}$ or L^{2-}

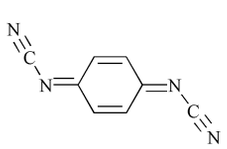

DCNQI

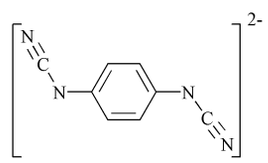

$dicyd^{2-}$

The complex $Cu(2,5\text{-}DM\text{-}DCNQI)_2$ (DM = dimethyl), that incorporates the radical anion of the DCNQI derivative, has been shown to possess metallic properties and conductivity which increase with decreasing temperature reaching a maximum of 5×10^5 S cm^{-1} at 3.5 K.[12] These properties are largely the result of the planarity of the radical anion of DCNQI and of its ability to form π stacks in the solid state.[13] These results have given a new impetus to the co-ordination chemistry of cyanamide ligands, largely investigated by Crutchley *et al.*[14] essentially with ruthenium, copper and nickel using a large number of ligands of the $dicyd^{2-}$ family.

In our exploration of transition metal co-ordination chemistry with cyanamido-squarate ligands, we have recently reported on copper complexes containing 3,4-bis(cyanamido)-cyclobutane-1,2-dione dianion (3,4-$NCNsq^{2-}$ or L^{2-}) and discussed the co-ordination properties of the cyanamido moiety.[15] In this present study, we examine the nature of the Ni–NCN bond in three nickel(II) complexes of the dianion L^{2-}.

DOI: 10.1039/b202085h

Experimental

Materials

All solvents and chemicals were reagent grade or better and used as received unless otherwise noted. The compounds squaric acid, cyanamide, imidazole (Him), tris(2-aminoethyl)-amine (tren), nickel(II) perchlorate hexahydrate and nickel(II) nitrate hexahydrate were purchased from Acros. The Na^+ and Ph_4P^+ salts of [3,4-bis(cyanamido)cyclobutane-1,2-dione dianion, L^{2-}], *i.e.* $Na_2L{\cdot}2H_2O$ and $(PPh_4)_2L{\cdot}4H_2O$ have been prepared according to a method adapted from Sprenger and Ziegenbein [16] and previously described.[15]

IR data (KBr disc)/cm^{-1} for $Na_2L{\cdot}2H_2O$: 3500–3260m, 2210m, 2163vs, 2120w (sh), 1790m, 1630s, 1557s, 1529s, 1450vs, 1215w, 1186w, 1022w, 1000w, 866w, 569m; for $(Ph_4P)_2L{\cdot}4H_2O$: 3434w (br), 3057w, 2167m (sh), 2120vs, 1768m, 1634s, 1585m, 1512vs, 1434vs, 1186w, 1162w, 1108vs, 994m, 852w, 761m, 723vs, 688s, 526vs. These values agree with those reported by Lunelli and Monari.[17]

CAUTION! Perchlorate salts of metal complexes with organic ligands are potentially explosive. Only a small amount of material should be prepared and handled with care.

Syntheses

$[Ni(Him)_4L(H_2O)]{\cdot}H_2O$ 1. An aqueous solution (10 cm^3) of a mixture of $Na_2L{\cdot}2H_2O$ (0.242 g, 1 mmol) and imidazole (Him) (1.36 g, 20 mmol) was added drop-wise to a water solution (10 cm^3) of $Ni(NO_3)_2{\cdot}6H_2O$ (0.291 g, 1 mmol). The yellow precipitate obtained was dissolved in 100 cm^3 of water. From slow evaporation of this solution, green crystals of **1** were obtained. (Found: C, 40.73; H, 3.64; N, 31.92. Calc. for $C_{18}H_{20}N_{12}O_4Ni$: C, 41.01; H, 3.82; N, 31.89%). IR data (KBr disc)/cm^{-1}: 3350 (br), 3144 (br), 2960w, 2864w, 2209s, 2188s, 2165 (sh), 2147vs, 1776m, 1645m, 1636m, 1541 (sh), 1522 (sh), 1502s, 1427s (br), 1329m.

$\{[Ni_2(Him)_2L_2(H_2O)_6]{\cdot}8H_2O\}_n$ 2. To prevent immediate formation of an insoluble precipitate, the synthesis was conducted in very dilute conditions. An aqueous solution (200 cm^3) of a mixture of $Ni(NO_3)_2{\cdot}6H_2O$ (0.145 g, 0.5 mmol) and imidazole (0.068 g, 1 mmol) was added to an aqueous solution (100 cm^3) of $Na_2L{\cdot}2H_2O$ (0.242 g, 1 mmol). Green crystals of **2** were obtained. (Found: C, 26.24; H, 4.30; N, 20.52. Calc. for $C_9H_{18}N_6O_9Ni$: C, 26.18; H, 4.39; N, 20.35%). IR data (KBr disc)/cm^{-1}: 3377–3128 (br), 2242 (sh), 2202s, 2178s, 2139 (sh) 1778m, 1649 (sh), 1631m, 1546 (sh), 1528s (br), 1461s (br), 1442 (sh), 1333m.

$[Ni(tren)L]_n$ 3. An aqueous solution (25 cm^3) of [Ni(tren)]-$[ClO_4]_2$ was obtained from nickel(II) perchlorate hexahydrate (0.366 g, 1 mmol) and tren (0.146 g, 1 mmol). To this solution was added a solution of $Na_2L{\cdot}2H_2O$ (0.484 g, 2 mmol) in water (10 cm^3): the blue solution turned brown. A small amount of brown precipitate appeared and, after filtration, violet crystals of **3** were obtained by slow evaporation at room temperature. (Found: C, 39.34; H, 4.66; N, 29.25. Calc. for $C_{12}H_{18}N_8O_2Ni$: C, 39.49; H, 4.97; N, 30.70%). IR data (KBr disc) cm^{-1}: 3311s, 2919w, 2228s, 2194s, 2175 (sh), 2163vs, 2130 (sh), 1777m, 1655m, 1622m, 1515s (br), 1440s (br).

Physical measurements

The complexes were isolated as air-stable crystals. Complexes **1** and **2** are soluble in dmf. Conductivity measurements showed that **3** (insoluble in dmf) is dissociated in water, the dissociation being associated with the fragmentation of the polymeric chain. UV-Visible spectra have been performed in dmf solution on a Cary 1E spectrophotometer. IR spectra were recorded in the solid state in KBr pellets using a 1760-X Perkin-Elmer Infrared Fourier Transform spectrometer. In the 2–300 K temperature range, magnetic susceptibility measurements were collected for powdered samples using a SQUID-based sample magnetometer on a QUANTUM Design Model MPMS instrument. $Hg[Co(NCS)_4]$ was used as a calibrant (susceptibility at 20 °C, 16.44×10^{-6} cm^3 mol^{-1}). The molar susceptibilities were corrected for diamagnetism using Pascal's constants. Corrections were estimated at -241.90×10^{-6}, -375.84×10^{-6} and -168.28×10^{-6} cm^3 mol^{-1} for all the atoms of **1**, **2** and **3** respectively. ESR spectra were recorded on a 9 GHz Bruker (ESP 300 E) instrument at ambient temperature for crystals and at 100 K for frozen solutions of dmf. Electrochemical measurements were carried out at room temperature with a home-made potentiostat controlled by a PC computer. The electrochemical cell (10 cm^3) was a conventional one with three electrodes: working electrodes, Pt (diameter 2 mm, EDI Tacussel) for rotating disk electrode experiments (LSV, linear sweep voltammetry), Pt (disk diameter: 0.5 mm and 50 μm) for cyclic voltammetry experiments (CV), different disk ultramicroelectrodes (Pt 10 μm Tacussel, glassy carbon 10 μm PAR, gold 25 μm) for steady-state experiments; counter electrode, Pt wire; and reference electrode, double junction SCE. The potential of the ferricinium ion/ferrocene couple is 0.486 V *versus* this reference [18] or 0.400 V *versus* the standard hydrogen electrode SHE.[19] The experiments were carried out in dmf–Bu_4NPF_6 0.1 M under an argon atmosphere; dmf (Acros, spectrosol) and Bu_4NPF_6 (Fluka, electrochemical grade) were used without further purification. The cyclic voltammetry was performed with the ohmic drop correction by positive feedback. The ohmic term R_u (uncompensated resistance) was first determinated by the current interrupt method.[20]

X-Ray data collection and structure determinations for 1, 2 and 3

The data were collected [21] at low temperature (T = 160 K) on a Stoe Imaging Plate Diffractometer System (IPDS), equipped with an Oxford Cryosystems cooler device, using graphite monochromated Mo-Kα radiation (λ = 0.71073 Å). For the three complexes, the data were collected with a crystal-to-detector distance of 70 mm, in the 2θ range of 3.3–52.1° with a ϕ oscillation movement (ϕ = 0.0–249.6°, $\Delta\phi$ = 1.3° for **1**, ϕ = 0.0–250.9°, $\Delta\phi$ = 1.3° for **2** and ϕ = 0.0–200.2°, $\Delta\phi$ = 1.4° for **3**). The structures were solved using direct methods [22] and refined [23] by full-matrix least-squares using the program SHELXL-97. Hydrogen atoms were introduced in calculated positions using a riding model (except those bonded to water molecules which were allowed to vary) with U_{iso} fixed at 20% higher than those of the connected atoms.

All non-hydrogen atoms were anisotropically refined. Refinements on F_o^2 were made for all reflections. Conventional R factors were based on F_o [$F_o > 4\sigma(F_o)$], with F_o set to zero for negative F_o^2. The atomic scattering factors and anomalous dispersion terms were taken from the standard compilation.[24]

Crystallographic data are summarized in Table 1.

CCDC reference numbers 181062–181064.

See http://www.rsc.org/suppdata/dt/b2/b202085h/ for crystallographic data in CIF or other electronic format.

Results and discussion

The most characteristic feature of the cyanamido compounds is a π electron system extended over the three NCN atoms (or more when this group is linked to an unsaturated moiety), which results in such stable anionic forms that cyanamido derivatives such as thio- and seleno-cyanates may be viewed as pseudo-halide ions. It is agreed that the π electron delocalisation results in a linear geometry of the NCN group and also in the planarity of the amido nitrogen surrounding. Two potential co-ordination sites may be viewed: the nitrile-nitrogen lone pair (end-on co-ordination) [25,26] or/and the amido nitrogen atom [27]

Table 1 Crystallographic data for $[Ni(Him)_4L(H_2O)]\cdot H_2O$ **1**, $\{[Ni_2(Him)_2L_2(H_2O)_6]\cdot 8H_2O\}_n$ **2** and $[Ni(tren)L]_n$ **3**

Compound	**1**	**2**	**3**
Formula	$C_{18}H_{20}N_{12}O_4Ni$	$C_9H_{18}N_6O_9Ni$	$C_{12}H_{18}N_8O_2Ni$
M	527.17	413.00	365.02
Colour	Green	Yellow–green	Purple
Crystal form	Rod	Parallelepiped	Rod
Crystal size/mm	0.65 × 0.22 × 0.10	0.50 × 0.35 × 0.20	0.75 × 0.25 × 0.25
Crystal system, space group	Triclinic, $P\bar{1}$	Triclinic, $P\bar{1}$	Orthorhombic, $P2_12_12_1$
a/Å	8.994(2)	6.966(5)	9.6957(7)
b/Å	10.836(2)	10.812(5)	11.3628(8)
c/Å	12.353(2)	11.699(5)	13.834(2)
α/°	70.39(2)	99.044(5)	
β/°	84.46(2)	90.794(5)	
γ/°	74.84(2)	105.502(5)	
U/Å^3	1094.6(2)	837.1(8)	1524.1(2)
Z	2	2	4
F(000)	544	428	736
T/K	160(2)	160(2)	160(2)
No. of measured reflections	10615	6228	9782
No. of independent reflections	3925	2273	2972
Final *R* indices [$I > 2\sigma(I)$]	$R1 = 0.0268$	$R1 = 0.0380$	$R1 = 0.0252$
	$wR2 = 0.0681$	$wR2 = 0.0836$	$wR2 = 0.0676$

(only a few cases of side-on co-ordination generating π complexes are known[28]). The majority of the cyanamido complexes involve end-on co-ordination and the bond angle between the cyanamido group and the metal ion is largely determined by the two resonance structures:

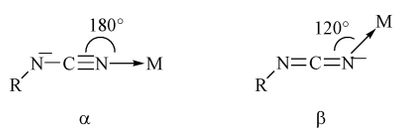

However, the contribution from both structures α and β occurs and experimental co-ordination angle values lie between 120 and 180°. We have recently described three cyanamido copper complexes,[15] two of them presenting an end-on co-ordination while in the third one, [Cu(tren)(3,4-NCNsq)], the co-ordination unusually occurs *via* the amido nitrogen atom with angles at this atom close to 120° as expected.

Lunelli *et al.*[29] have provided evidence, by means of IR spectroscopy, that the two conformers A and B of the dianion L^{2-} coexist in solution with the predominant form being A. In the solid state, the form B will be predominant in small cation salts while the form A is obtained with the bulkier Tl^+ or PPh_4^+. The IR spectra of a metallic complex may allow differentiation of forms A from B in the co-ordinated ligand. To date, only the form A of L^{2-} has been identified by crystallography as well in salts[17] as in copper complexes.[15]

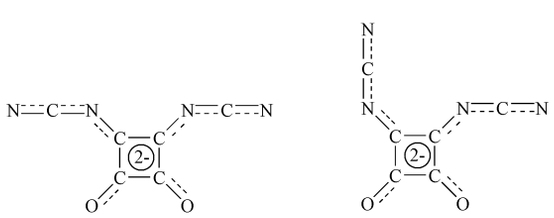

Selected bond lengths and angles from the structural determinations of $[Ni(Him)_4L(H_2O)]\cdot H_2O$ **1**, $\{[Ni_2(Him)_2L_2(H_2O)_6]\cdot 8H_2O\}_n$ **2** and $[Ni(tren)L]_n$ **3** are given in Tables 2, 3 and 4 respectively.

Crystal structure of $[Ni(Him)_4L(H_2O)]\cdot H_2O$ 1

A view of the molecule, along with the numbering scheme, is shown in Fig. 1 (see Table 2 for selected bond lengths and angles). The compound consists of discrete $[Ni(Him)_4(3,4\text{-}NCNsq)(H_2O)]$ mononuclear molecules and one water molecule in the lattice. The geometry around the nickel(II) atom is slightly distorted octahedral with the co-ordination polyhedron defined by four nitrogen atoms of four Him molecules, a water molecule and one nitrogen atom of one nitrile group of the L^{2-} ion. The best equatorial plane is comprised of atoms N11, N21, N41 of three Him molecules and O1w of the water molecule. The metal atom only exhibits a 0.0132(2) Å deviation from this plane. The Ni–N (Him) distances are practically equivalent [from 2.081(2) to 2.111(2) Å]. Concerning the ligand L^{2-}which lies as the A conformer, only one of the NCN groups is co-ordinated to the metal. Free anionic cyanamide ligands are expected to be planar because of the important π delocalised system; in the complex, the squarate ring including oxygen atoms is almost planar and the co-ordinated and unco-ordinated NCN groups lie approximately in this plane (the maximum dihedral angle being 3° between the squarate ring and N3C6N4). The co-ordinated cyanamido group adopts an almost linear co-ordination mode with an angle Ni–N1–C1 of 176.8(2)°. Associated with this linkage, the C–N (nitrile) bond length [1.157(2) Å] is shorter than the unco-ordinated one [1.163(2) Å]. This corresponds, as expected, to an increase of the nitrile bond

Table 2 Selected bond lengths (Å) and angles (°) for $[Ni(Him)_4L(H_2O)]\cdot H_2O$ **1** with e.s.d.s in parentheses

Ni–N41	2.081(2)	Ni–N11	2.091(2)
Ni–N21	2.099(2)	Ni–N31	2.111(2)
Ni–N1	2.119(2)	Ni–O1w	2.125(2)
N1–C1	1.157(2)	C1–N2	1.314(2)
N2–C2	1.344(2)	N4–C6	1.163(2)
C6–N3	1.309(2)	N3–C3	1.334(2)
C2–C3	1.414(2)	C2–C5	1.453(2)
C4–C5	1.498(2)	C4–C3	1.469(2)
C5–O1	1.239(2)	C4–O2	1.229(2)
N41–Ni–N21	91.87(6)	N11–Ni–N21	92.63(6)
N41–Ni–N31	90.11(6)	N11–Ni–N31	91.28(6)
N21–Ni–N31	91.89(6)	N41–Ni–N1	90.43(6)
N11–Ni–N1	87.97(6)	N21–Ni–N1	90.80(6)
N41–Ni–O1w	86.35(6)	N11–Ni–O1w	89.16(6)
N31–Ni–O1w	88.05(6)	N1–Ni–O1w	89.29(6)
Ni–N1–C1	176.8(2)	N1–C1–N2	172.5(2)
C1–N2–C2	118.5(2)	N2–C2–C3	132.1(2)
N2–C2–C5	136.0(2)	N4–C6–N3	173.4(2)
C6–N3–C3	117.3(2)	N3–C3–C2	132.8(2)
N3–C3–C4	135.8(2)	C4–C5–C2	88.7(2)
C5–C2–C3	91.9(2)	C2–C3–C4	91.3(2)
C3–C4–C5	88.1(2)		

Table 3 Selected bond lengths (Å) and angles (°) for $\{[Ni_2(Him)_2L_2(H_2O)_6]\cdot 8H_2O\}_n$ **2** with e.s.d.s in parentheses

Ni1–N5	2.059(3)	Ni1–O1w	2.105(3)
Ni1–N2	2.080(4)	Ni2–O2w	2.049(3)
Ni2–O3w	2.080(3)	Ni2–N4	2.019(4)
C1–C2	1.444(6)	C2–C3	1.482(6)
C3–C4	1.474(6)	C4–C1	1.425(6)
C2–O1	1.247(5)	C3–O2	1.240(5)
C1–N1	1.332(5)	N1–C5	1.322(5)
C5–N2	1.155(5)	C4–N3	1.314(5)
N3–C6	1.316(7)	C6–N4	1.187(7)
N2–Ni1–N5	90.0(2)	N2–Ni1–N5[1]	90.0(2)
N2–Ni1–O1w	90.1(2)	N2–Ni1–O1w[1]	89.9(2)
N5–Ni1–O1w	90.3(2)	N5–Ni1–O1w[1]	89.7(2)
N4–Ni2–O2w	92.3(2)	N4–Ni2–O2w[2]	87.7(2)
N4–Ni2–O3w	91.6(2)	N4–Ni2–O3w[2]	88.4(2)
O2w–Ni2–O3w	88.4(2)	O2w–Ni2–O3w[2]	91.6(2)
Ni1–N2–C5	164.1(3)	N2–C5–N1	170.8(4)
C5–N1–C1	119.8(4)	N1–C1–C2	131.2(4)
N1–C1–C4	137.4(4)	C1–C2–C3	89.8(3)
C1–C2–O1	134.4(4)	C2–C3–C4	88.0(3)
C2–C3–O2	136.5(4)	C3–C4–C1	90.8(3)
C3–C4–N3	138.2(4)	C4–N3–C6	122.6(4)
N3–C6–N4	171.8(5)	C6–N4–Ni2	160.6(4)

Symmetry operations: [1] $-x, -y+1, -z$; [2] $-x, -y+2, -z-1$.

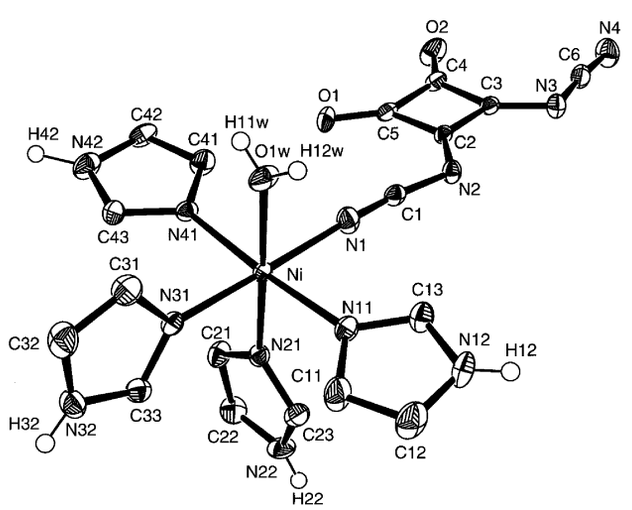

Fig. 1 Molecular structure of $[Ni(Him)_4L(H_2O)]\cdot H_2O$ **1**.

character for the co-ordinated nitrile group. The end-on co-ordination mode of the ligand L^{2-} in complex **1** may be compared to that of the ligand 2-Clpcyd$^-$ obtained in the monomer complex [Ni(imd)(2-Clpcyd)] where imd$^-$ = 1,3-bis(2-pyridylimino)isoindolinato anion and 2-Clpcyd$^-$ = 2-chlorophenylcyanamido anion.[25] While the C–N (nitrile) bond lengths are similar in the two complexes, the co-ordination is stronger in [Ni(imd)(2-Clpcyd)] [Ni–N = 1.874(10) Å instead of 2.119(2) Å in **1**] associated with a Ni–N–C angle value of 161.8(10)°.

The C–C distances in the squarate ring, in the range 1.414(2)–1.498(2) Å, are indicative of a π delocalised system, the shortest one being located between the two NCN groups.

The geometry of the imidazole ligand is similar to previously reported data[30] and will therefore not be discussed in detail.

A large hydrogen bond network involves hydrogen atoms of the water molecules and the NH group of the Him rings with the oxygen and nitrogen atoms of the ligand L^{2-} (excepted N1 which is bonded to the nickel atom) and the oxygen atom of the unco-ordinated water molecule.

Crystal structure of $\{[Ni_2(Him)_2L_2(H_2O)_6]\cdot 8H_2O\}_n$ 2

A view of the compound, along with the numbering scheme, is shown in Fig. 2 (see Table 3 for selected bond lengths and angles). The structure of **2** consists of two different square-planar Ni(II) units $[Ni(Him)_2(H_2O)_2]$ and $[Ni(H_2O)_4]$ linked by L^{2-} bridges to form infinite chains and eight water molecules in the lattice. In each chain, the two different nickel atoms Ni1 and Ni2 lie in approximate octahedral co-ordination geometry and provide two crystallographic inversion centres. Ni1 is co-ordinated to two water molecules, two nitrogen atoms of two Him ligands and two nitrogen atoms of two L^{2-} ions. The other metal atom Ni2 is co-ordinated to four water molecules and two nitrogen atoms of two L^{2-} ions. So, each L^{2-} ion bridges the metal atoms Ni1 and Ni2 by its two cyanamido functions, and for the first time, the B conformer is identified by X-ray crystallography. In this conformer, two different NCN groups can be labelled as NCN(1) and NCN(2).

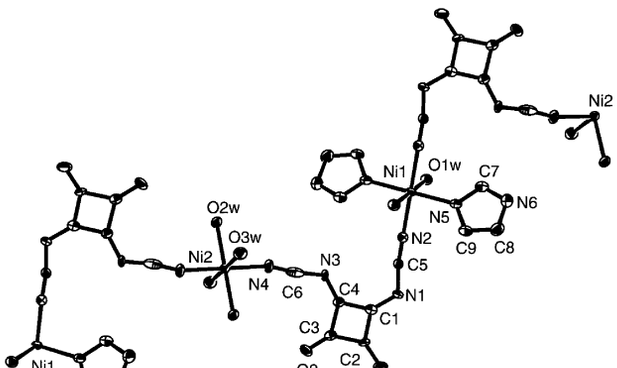

Fig. 2 Molecular structure of $\{[Ni_2(Him)_2L_2(H_2O)_6]\cdot 8H_2O\}_n$ **2**.

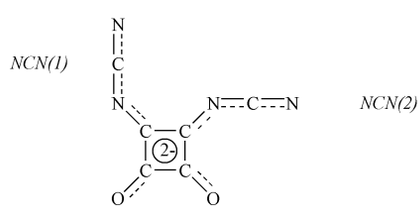

It can be noted that the Ni1 atom is co-ordinated to two NCN(1) groups when the Ni2 atom is co-ordinated to two NCN(2) groups but this characteristic has no effect on the Ni–N distance values. The two NCN groups are end-on co-ordinated by the nitrile nitrogen with angles deviating from the linear mode ideal angle [Ni2–N4–C6 = 160.6(4) and Ni1–N2–C5 = 164.1(3)°]. As expected, the C–N (nitrile) bonds lengths [C6–N4 = 1.187(7) and C5–N2 = 1.155(5) Å] are shorter than those of the free dianion. The squarate ring including the oxygen atoms is almost planar, however the two NCN groups deviate significantly from this plane and are twisted in opposite directions, the deviations being 14.69° for N1C5N2 and −11.08° for N3C6N4. The C–C distances in the squarate ring are in the range 1.425(6)–1.482(6) Å, characteristic values for a delocalised π system. The shortest distance corresponds to the C–C bond located between the two NCN groups. The C–O distances are normal for carbonyl groups.

The hydrogen bond network involves as donor groups, all the water molecules (bonded and non-bonded) and the N–H groups of the imidazole ligands, and as acceptors, the oxygen atoms and the amido nitrogen atoms of the ligand L^{2-} and the oxygen atoms of the water molecules.

The geometry of the imidazole ligand is similar to previously reported data.[30]

Crystal structure of $[Ni(tren)L]_n$ 3

A view of the molecule, along with the numbering scheme, is shown in Fig. 3 (see Table 4 for selected bond lengths and

Table 4 Selected bond lengths (Å) and angles (°) for $[Ni(tren)L]_n$ **3** with e.s.d.s in parentheses

Ni–N2	2.039(2)	Ni–N4	2.151(2)
Ni–N5	2.108(2)	Ni–N6	2.131(2)
Ni–N7	2.098(2)	Ni–N8	2.098(2)
N2–C5	1.151(3)	C5–N1	1.317(3)
N1–C1	1.336(3)	N4–C6	1.161(3)
C6–N3	1.314(3)	N3–C4[1]	1.326(3)
C1–C2	1.461(3)	C2–C3	1.496(3)
C3–C4	1.477(3)	C1–C4	1.424(3)
C2–O1	1.233(3)	C3–O2	1.223(3)
N5–C7	1.479(3)	C7–C8	1.520(3)
C8–N6	1.490(3)	N5–C9	1.483(3)
C9–C10	1.518(3)	C10–N7	1.485(3)
N5–C11	1.486(3)	C11–C12	1.521(4)
C12–N8	1.479(3)		
N2–Ni–N7	92.60(8)	N2–Ni–N8	89.59(8)
N7–Ni–N8	95.77(8)	N7–Ni–N5	83.90(8)
N8–Ni–N5	83.28(8)	N2–Ni–N6	101.98(8)
N8–Ni–N6	93.75(7)	N5–Ni–N6	82.81(7)
Ni–N2–C5	162.2(2)	N2–C5–N1	170.8(3)
Ni–N4–C6	153.0(2)	N4–C6–N3	174.1(2)
C5–N1–C1	120.4(2)	C6–N3–C4[1]	116.1(2)
C1–C4–N3[2]	132.9(2)	C3–C4–N3[2]	136.1(2)
C4–C1–N1	139.6(2)	C2–C1–N1	128.6(2)
C1–C4–C3	91.0(2)	C4–C3–C2	88.2(2)
C3–C2–C1	88.8(2)	C2–C1–C4	91.7(2)

Symmetry operations: [1] $x - 1/2, -y + 1/2, -z + 1$; [2] $x + 1/2, -y + 1/2, -z + 1$.

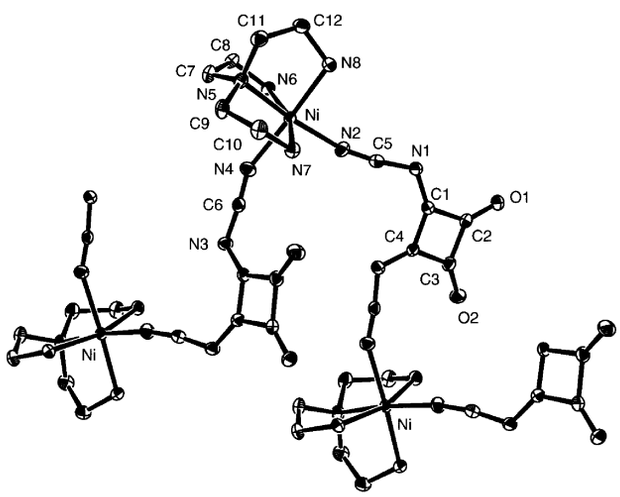

Fig. 3 Molecular structure of $[Ni(tren)L]_n$ **3**.

angles). It may be underlined here that we have recently obtained a copper(II) complex with a similar raw formula [Cu(tren)L],[15] but these two complexes are not isostructural. The copper complex is a monomer and the metal atom is penta-co-ordinated to the four nitrogen atoms of the tren ligand and to one amido nitrogen atom of the L^{2-} ligand. The structure of **3** is made of infinite chains of [Ni(tren)(3,4-NCNsq)] units. The nickel(II) ions lie in an approximate octahedral co-ordination geometry, each of them being co-ordinated to the four nitrogen atoms of the tren ligand and to two nitrogen atoms of two different L^{2-} ions. So, the L^{2-} ion provides a bridge between the metal atoms by way of its two cyanamido moieties. The best equatorial plane around the metal atom is constituted by the two nitrogen atoms of the two L^{2-} ions (N2, N4) and by two nitrogen atoms of the tren ligand (N5, N8). The angles at the metal atom by the tetradentate tren ligand are in the range 82.81(7)–95.77(8)°. The Ni–$N_{terminal}$ (tren) bonds are in the range 2.098(2)–2.131(2) Å. Most often, the Ni–$N_{central}$ (tren) bond has been found to be either the longest or the shortest of the Ni–N bonds.[31] But, in this case, this bond has an intermediate length [2.108(2) Å]. At the same metal atom, the two Ni–N (nitrile) distances are strongly different, the shortest being 2.039(2) Å for Ni–N2 and the largest being 2.151(2) Å for Ni–N4. So, one ligand is strongly co-ordinated by N2 and the other one is poorly co-ordinated by N4. Associated with these distances, the Ni–N2–C5 angle is closer to 180° [162.2(2)°] than the Ni–N4–C6 one [153.0(2)°].

In this complex, the ligand L^{2-} is also observed in the B conformation. It is affected by complexation and one may notice a shortening of the terminal C–N bond [1.21(4) Å in the free dianion and 1.151(3) Å and 1.161(3) Å in the complex] which corresponds to an increase of the nitrile bond-character. The squarate ring including oxygen atoms is almost planar, however the two NCN groups deviate very significantly from this plane and are twisted in the same direction, the deviation being 17.6° for C1N1C5N2 and 19.9° for C4N3C6N4. The C–C distances in the squarate ring, in the range 1.424(3)–1.496(3) Å, are indicative of a π delocalised system, the shortest one being situated between the two NCN groups.

The hydrogen bond network involves the nitrogen atom N6 of the tren ligand, the co-ordinated nitrogen atom of one of the nitrile groups N4, the two amido nitrogen atoms N1 and N3 and the oxygen atom O1 of the ligand L^{2-}.

IR and electronic spectroscopies

The IR spectra of cyanamides and related diimides[32–35] present an absorption band in the range 2150–2100 cm^{-1} assigned to N=C=N stretching. For the cyanamido squarate ions, the ν(N=C=N) is also observed in this area. The work of Lunelli *et al.*[29] associated with our recent results[15] show that the solid state spectra of L^{2-} largely depend on the nature of the prevalent conformer A or B. For the form A, the ν(N=C=N) band is observed at 2120 cm^{-1} according to the spectra of Tl^+ and PPh_4^+ salts.[29] In form B, the characteristic peak is found at 2160 cm^{-1} according to the spectra of the Na^+ salt.[15,29]

In the three nickel(II) complexes, co-ordination of the cyanamido ligand occurs *via* the nitrogen atom of the nitrile group (end-on co-ordination). This may be associated, as for nitrile ligands, with a positive shift $\Delta\nu$(N=C=N) from 20 to 40 cm^{-1}.[35] In **1**, the ligand takes up the A conformation with only one of the NCN groups co-ordinated to the metal atom. The main ν(N=C=N) band is observed at 2147 cm^{-1} with a positive shift in comparison with the free dianion ($\Delta\nu$ = + 27 cm^{-1}). A continuous absorption at 3600–3200 cm^{-1} with a sharp maximum at 3350 cm^{-1} is attributable to the presence of an aqua ligand with extensive hydrogen bonding. In complexes **2** and **3**, the ligand is present as the B conformer. In the spectra of **2**, two strong bands are observed at 2202 and 2178 cm^{-1} with shoulders at 2242 and 2139 cm^{-1}; a positive average shift may be calculated *versus* the free dianion frequency ($\Delta\nu_{av}$ = + 27 cm^{-1}). In the spectra of **3**, the main absorption is observed at 2163 cm^{-1}, an unexpected value for a co-ordinated ligand. The large hydrogen bond network implies that the nitrogen atoms of the NCN groups may be responsible for this large area overlap.

Absorptions at 1776 (**1**), 1778 (**2**) and 1777 (**3**) cm^{-1} correspond to ν(C=O) bands of the squarate ring. These bands are affected by complexation (1790 cm^{-1} in form A, 1768 cm^{-1} in form B for the free ligand), however they are not related to the occurrence of the different conformers observed in the complexes. The bands at *ca.* 1630 cm^{-1} associated with the strong and broad absorptions centred at 1502 (**1**), 1528 (**2**) and 1515 (**3**) cm^{-1} are assigned to a combination of C=O and C=C stretching vibrations. This last band is observed at 1529 cm^{-1} in L^{2-} and is characteristic of $C_nO_n^{2-}$ salts since it was found at *ca.* 1500 cm^{-1} in the spectrum of $K_2C_4O_4$.[36]

The π–π* absorption band in the spectra of the dianion L^{2-} has already been reported by Kohler *et al.*[37] (316 nm in methanol for the disodium salt), and Lunelli *et al.*[29] (in dmf,

385 nm for the disodium and 323 nm for the dithallium salts). These last authors ascribe these two different values to the presence, even in solution, of the two conformers A and B. However, we have obtained, for dmf solution measurements, the same value of 324 nm (log $\varepsilon = 4.52$) for the Na^+ and PPh_4^+ salts. This result is not surprising since the electronic spectra are performed at very low concentration (10^{-5} mol L^{-1}), so only the predominant form A is observed.

The electronic spectra of complexes **1** and **2** are dominated by the π–π* transition of the ligand and the λ_{max} is not affected by complexation. The low energy bands, arising from a ligand field transition (d–d) are at 445, 612 and 1077 nm for **1**, 657 and 1113 nm for **2** (the first band is hidden by the broad π–π* absorption band) with ε values from 10 to 30. These values are consistent with a quasi-octahedral geometry around the nickel atom. On the basis of O_h symmetry, the maxima are assigned to transitions from the $^3A_{2g}$ ground state to $^3T_{2g}$, $^3T_{1g}(F)$ and $^3T_{1g}(P)$ excited states.

Magnetic data

The μ_{Ni} *vs.* temperature data for complexes **1**, **2** and **3** are shown in Fig. 4.

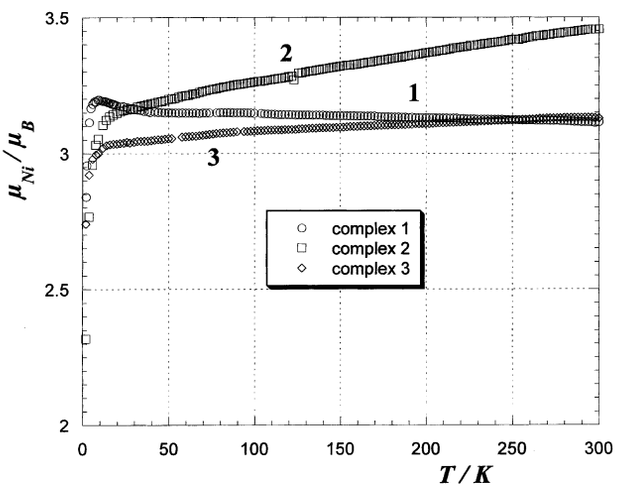

Fig. 4 Plots of μ_{Ni} *vs.* temperature for complexes **1**, **2** and **3**.

For the monomer complex **1**, the variation of the reciprocal molar magnetic susceptibility data *versus* temperature is described by a Curie–Weiss law, *i.e.* $\chi_M = C / (T - \theta)$ with $\theta = -1.29$ K and $C = 1.22$ cm^3 K mol^{-1}. The magnetic moment μ_{eff} was found to be 3.12 μ_B at 300 K, slightly higher than the spin only value (2.83 μ_B) as usually observed for octahedral Ni(II) due to the second order spin–orbit coupling.[38] This value slightly increases to a maximum of 3.20 μ_B at 11 K and decreases rapidly at lower temperatures down to 2.84 μ_B due to the zero-field splitting effects of the Ni(II) ion. The increase in μ_{eff} values from room temperature down to 11 K may be related to a weak ferromagnetic interaction as found between the Ni^{2+} ions in dinuclear units.[39–41] This unexpected result for a monomer complex was checked by the use of several samples. ESR measurements on crystals of **1** are consistent with the presence of an $S = 1$ isolated Ni(II) ion ($g_1 = 2.42$, $g_2 = 2.15$, $g_3 = 1.92$). So, the observed magnetic behaviour may be related to a ferromagnetic coupling with a small amount of isolated Ni^{2+} even if the possibility of an intermolecular interaction must not be discarded.

For the polymeric complexes **2** and **3**, the magnetic moments (3.46 μ_B for **2**, 3.13 μ_B for **3** at 300 K) correspond to that usually observed for octahedral Ni(II) and are higher than the spin only value usually observed. In a first approximation, the variation of the effective magnetic moment within the 2–300 K domain agrees with that expected for essentially non-interacting nickel(II) ions with zero-field splitting effects.[42] The high temperature data obeyed the Curie–Weiss law, yielding $C = 1.51$ cm^3 K mol^{-1} and $\theta = -10.37$ K for **2**, $C = 1.23$ cm^3 K mol^{-1}and $\theta = -2.96$ K for **3**.The temperature dependence of the susceptibility of infinite isotropic Heisenberg chains, in the case $S = 1$, may be fitted by the following analytical expression [eqn. (1)][43] which is only valid for an antiferromagnetic coupling ($J < 0$):

$$\chi_{chain} = (N\beta^2g^2/kT)[(2 + 0.0194X + 0.777X^2)/(3 + 4.346X + 3.232X^2 + 5.834X^3)] \quad (1)$$

with $X = |J|/kT$. The least-squares fitting of the experimental data led to the exchange coupling constants $J = -2.98$ cm^{-1} for **2** and -1.17 cm^{-1} for **3**.

A fit with unique spin Hamiltonian parameters D, $g_{||}$ and $g_\perp$ is difficult to obtain; so the zero-field splitting parameter D was calculated from the very low temperature limit equation [eqn. (2)].[4]

$$\chi_M = 4N\beta^2g_\perp^2/3D \quad (kT \ll D) \quad (2)$$

To a first approximation we assumed $g_\perp \approx g_{||}$, since octahedrally surrounded Ni(II) ions generally show isotropic g values. From the high temperature limit equation [eqn. (3)]

$$\chi_M = 2N\beta^2g^2/3kT \quad (kT \gg D) \quad (3)$$

we calculated $g = 2.4$ for **2** and 2.2 for **3** $\approx g_\perp$. When these values for $g_\perp$ were substituted in eqn. (2), the D values were found to be $+2.8$ cm^{-1} for **2** and $+4.0$ cm^{-1} for **3**. This indicates that weak couplings occur between the nickel atoms in complexes **2** and **3**, in agreement with the X-ray structural data giving 6.966 Å for the Ni–Ni shortest distances in **2** and 7.144 Å in **3**.

Electrochemistry

In the electroactivity domain of dmf–Bu_4NPF_6, the cyclic voltammograms of the two complexes **1** and **2** present the same shape (Figs. 5 and 6) and are compared to those of the free ligand L^{2-}. As already mentioned, the voltammogram of the free ligand shows two successive monoelectronic oxidations:[29] The first step corresponds to the oxidation of the dianion into the radical-anion ($E_{1/2} = 0.43$ V),

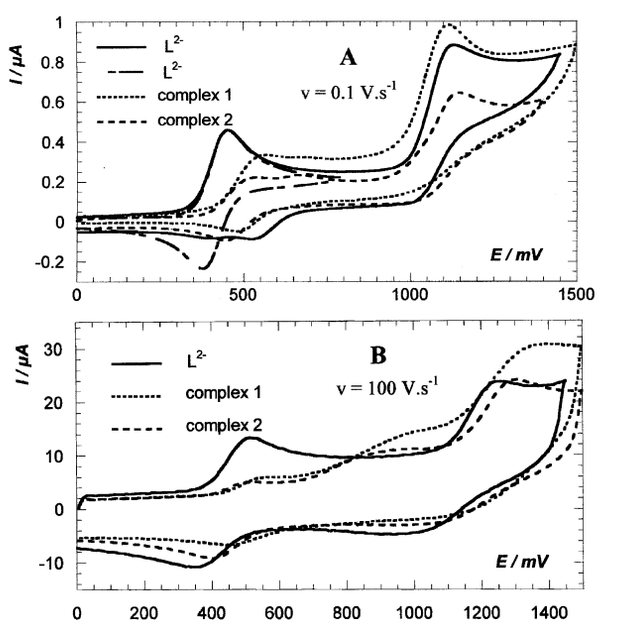

Fig. 5 Cyclic voltammograms at a Pt disk electrode (diameter 0.5 mm) in 0.1 M dmf–Bu_4NPF_6, potential scan speeds 0.1 V s^{-1} in **A** and 100 V s^{-1} in **B** (potential scanning starting at 0 V towards anodic potential and back to 0 V): (—) and (- · -) L^{2-}, 1.0 mM; (· · ·) complex **1**, 1.0 mM; (- - -) complex **2**, 1.0 mM.

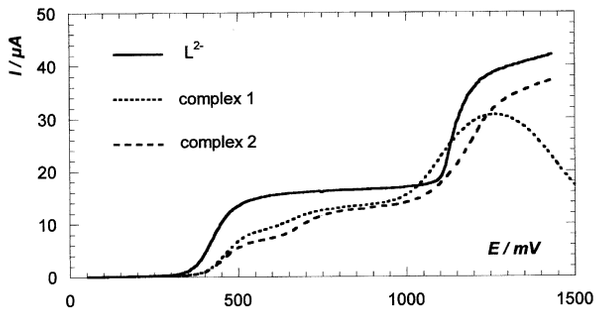

Fig. 6 Voltammograms at a rotating Pt disk electrode (diameter 2 mm) in 0.1 M dmf–Bu_4NPF_6, electrode rotation speed 2000 r.p.m. (—) L^{2-}, 1.0 mM; (· · ·) complex **1**, 1.0 mM; (- - -) complex **2**, 1.0 mM.

$$L^{2-} \rightleftharpoons L^{-\bullet} + e^- \quad \text{system 1}$$

The second step corresponds to the oxidation of the radical-anion into the neutral form ($E_{1/2}$ = 1.13 V),

$$L^{-\bullet} \rightleftharpoons L + e^- \quad \text{system 2}$$

Moreover, an irreversible reduction process is observed (E_p = −1.78 V for a potential scan speed of 0.1 V s^{-1}). Taking into account the monoelectronic oxidation transfer, the reduction peak current is twice the oxidation peak current which means that the reduction process is bielectronic and yields a tetra-anion:

$$L^{2-} + 2e^- \rightleftharpoons L^{4-} \quad \text{system 3}$$

This irreversible process is still present in the voltammograms of the complexes but badly defined. No evidence of Ni^{2+} reduction is given. The study has been restricted to the oxidation phenomena.

The electrooxidation of the ligand is not so simple (Fig. 5). The voltammograms show the two redox systems 1 and 2 which are complicated by chemical reactions.

As concerns system 2, it appears that the ratio of the oxidation peak currents I_{p_2}/I_{p_1} is always higher than 1 but decreases when the potential scan speed is enhanced and this system does not, at present, lookto be a reversible process. Taking into account the first monoelectron process, system 2 consists of a monoelectron transfer followed by a chemical reaction and a further electrooxidation to yield an apparent electron exchange higher than 1. At a potential scan speed of 100 V s^{-1} (Fig. 5B), the voltammograms present the shape of a simple EE mechanism in which the first step is rapid and the second step is slower with a dissymmetric transfer coefficient around 0.3.[44,45] The second electron transfer on the ligand induces a loss of π delocalisation as in the electrooxidation of the squarate dianion $C_4O_4^{2-}$ into the instable tetraacetone C_4O_4.[46] This structural change results in a slow heterogeneous rate constant and a dissymmetric transfer coefficient. At low potential scan speed, the unstable neutral compound L is further oxidized which gives to the voltammogram a shape of an irreversible process.

Concerning system 1 (Fig. 5), the shape of the voltammogram depends on the potential scan speed and on the potential scan. When the potential scan is restricted to system 1 (Fig. 5A, curve - - -), the first electron transfer appears reversible whatever the potential scan speed is. On the contrary, when scanning the potential between 0 and 1.5 V, the backward peak of the first system is split into two peaks (Fig. 5A, curve —). By increasing the potential scan speed (>9 V s^{-1}), the voltammogram has the look of a reversible system (Fig. 5B). This was interpreted by the presence of the two conformers A and B engaged in a square scheme mechanism:[29]

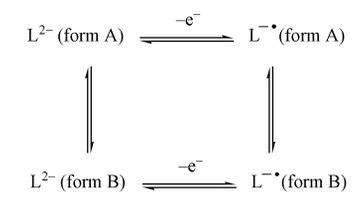

Under the dianion state, A is predominant while under the radical anion state the ratio form A/form B is around 70/30, as obtained by ESR measurements.[29]

The electrochemical behaviour of this ligand is similar that of the 1,4-dicyanamidobenzene dianion ($dicyd^{2-}$).[14] It can be pointed out that the potential domain of the radical anion states are of the same order (around 0.7 V) but the ligand L^{2-} requires more anodic potentials to be oxidized.

The voltammograms of the complexes **1** and **2** (Fig. 5 and 6) are different from the ones of the free ligand. The first electron transfer (system 1) is split into two processes: by cyclic voltammetry, two oxidation peaks are observed ($E_p \approx 0.5$ and 0.65 V) and under hydrodynamic conditions, two waves replace the oxidation wave of system 1. Around 1 V, the oxidation process (system 2) is still present for the two complexes, only a slight displacement of the peak potentials is observed. At a rotating electrode, electrode fouling is noticeable when the potential goes beyond 1 V.

When the potential scan speed is increased (Fig. 5B), the peak corresponding to system 1 (free ligand) vanishes while the peak corresponding to system 2 is little affected. Taking into account the variations of the cyclic voltammograms with the potential scan speed (from 0.01 up to 1000 V s^{-1}) and with the help of digital simulations,[44] the oxidation of the Ni complexes (named NiL) may be represented by a square scheme:

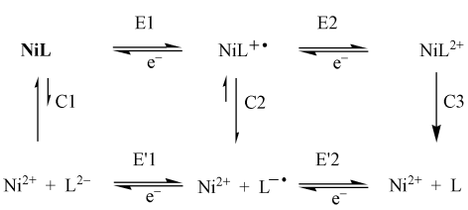

According to conductimetric measurements, the complexes in solution are under their neutral undissociated form **NiL**. The electrochemical oxidation of the complexes follows two pathways, which depends on the time scale of the experiment (potential scan speed). Using a low potential scan speed, the main pathway is C1–E′1–E′2: dissociation of the ligand and then oxidation. When the potential scan speed is increased, reaction C1 is frozen and the pathway E1–C2–E′2 is observed: direct oxidation of the ligand bound to the nickel. Reaction C1 is also frozen by decreasing the temperature: the signal at potential E1 is increased *versus* the one at E′1. Whatever the potential scan speed is, no backward peak has been observed for E1 transfer (Fig. 5): reaction C2 is very fast. The oxidized form $NiL^{+\bullet}$ is unstable because the unpaired electron is mainly located on the NCN moiety[29] which loses its co-ordinating ability. The anodic potential displacement from E′1 to E1 is in agreement with the effect of high complexation of the L^{2-} dianion[47] but also with a poorer complexation of the radical anion. Moreover, after electrolysis on the first step, ESR spectra on a frozen dmf solution showed the signal of the radical anion $L^{-\bullet}$. This was not the case in complexes of copper or cobalt with croconate violet in which co-ordination involves the oxygen atoms.[48,49] The radical anion of croconate violet presents an unpaired electron more or less located on the dicyanomethylene groups and is still co-ordinated to the metal by the oxygen atoms.

Taking into account these results, the electrochemical behaviour of the two complexes may be compared. The voltam-

mograms under stationary conditions present the same shape (Fig. 6). Assuming a total exchange of one electron for the first two steps, the currents are lower than in the free ligand. This is consistent with the lower diffusion coefficients of the complexes than the one of L^{2-} dianion. Moreover, the currents of the two complexes are of the same order of magnitude. This implies that the polymer (complex **2**) is dissociated in neutral species, because its null conductivity, with a diffusion coefficient close to that of complex **1**: that is monomers or dimers. Cyclic voltammetry shows that reaction C1 is faster in complex **1** than in complex **2**: reaction C1 becomes frozen at 4 V s^{-1} in complex **2** and at 16 V s^{-1} in complex **1**. This may be explained by the number of imidazole ligands in the co-ordination sphere of Ni^{2+}.

Because of electrode fouling occurring on the second oxidation, it is difficult to compare the two complexes. At the potential scan speed used, no backward peak was found for the reverse E1 electron transfer which means that the occurrence of E2 electron transfer is uncertain. However that may be, the radicalar complexes $NiL^{+\bullet}$ are unstable and cannot be isolated. According to the square scheme of NiL complex electrooxidation, it appears that the L^{2-} dianion belongs to the family of electrochemically switchable molecules.[50] Under the dianion state, the ligand is co-ordinated to the Ni^{2+} ion while upon oxidation into the $L^{-\bullet}$ radical anion Ni^{2+} is released. So the cation binding of this ligand L^{2-} can be electromodulated and work is in progress for specific cation recognition.

Acknowledgements

We thank A. Mari (Laboratoire de Chimie de Coordination, Toulouse) for magnetic and ESR measurements and E. Clark (ERASMUS student) for her participation in the syntheses.

References and notes

1 B. C. Gerstein and M. Habenschuss, *J. Appl. Phys.*, 1972, **43**, 5155.
2 M. Habenschuss and B. C. Gerstein, *J. Chem. Phys.*, 1974, **61**, 852.
3 A. Weiss, E. Riegler and C. Robl, *Z. Naturforsch., Teil B*, 1986, **41**, 1329.
4 J. A. C. Van Ooijen, J. Reedijk and A. L. Spek, *Inorg. Chem.*, 1979, **18**, 1184.
5 A. Weiss, E. Rriegler, I. Alt, H. Böhme and Ch. Robl, *Z. Naturforsch., Teil B*, 1986, **41**, 18.
6 R. Soules, F. Dahan, J. P. Laurent and P. Castan, *J. Chem. Soc., Dalton Trans.*, 1988, 587.
7 I. Castro, M. L. Calatayud, J. Sletten, F. Lloret and M. Julve, *J. Chem. Soc., Dalton Trans.*, 1997, 811.
8 R. West and D. L. Powell, *J. Am. Chem. Soc.*, 1963, **85**, 2577.
9 (*a*) H. E. Sprenger and W. Ziegenbein, *Angew. Chem., Int. Ed. Engl.*, 1967, **6**, 553; (*b*) H. E. Sprenger and W. Ziegenbein, *Angew. Chem., Int. Ed. Engl.*, 1968, **7**, 530.
10 A. J. Fatiadi, in *Oxocarbons*, R. West, ed., Academic Press, New York, 1980.
11 The name of compounds including the NCN group is not well established in the literature due to the number of conceivable isomers. The most common names are cyanimide, cyanimine, carbodiimide, cyanamide, cyanoimine, cyanoquinonediimine (CNQI). We have adopted from R. Crutchley, the term of "cyanamide" and the term of "cyanamido" for the deprotonated forms.
12 A. Aumüller, P. Erk, G. Klebe, S. Hünig, J. U. von Schütz and H. P. Werner, *Angew. Chem., Int. Ed. Engl.*, 1986, **25**, 740.
13 R. Kato, H. Kobayashi and A. Kobayashi, *J. Am. Chem. Soc.*, 1989, **111**, 5224.
14 R. J. Crutchley, *Coord. Chem. Rev.*, 2001, **219–221**, 125 and references therein.
15 P.-L. Fabre, A. M. Galibert, B. Soula, F. Dahan and P. Castan, *J. Chem. Soc., Dalton Trans.*, 2001, 1529.
16 (*a*) H. E. Sprenger and W. Ziegenbein, *Angew. Chem., Int. Ed. Engl.*, 1967, **6**, 553; (*b*) H. E. Sprenger and W. Ziegenbein, *Angew. Chem., Int. Ed. Engl.*, 1968, **7**, 530.
17 B. Lunelli and M. Monari, *Z. Naturforsch., Teil B*, 1989, **44**, 169.
18 D. Ranchet, J.-B. Tommasino, O. Vittori and P.-L. Fabre, *J. Solution Chem.*, 1998, **27**, 979.
19 A. M. Bond, E. A. McLennan, R. S. Stojanovic and F. G. Thomas, *Anal. Chem.*, 1987, **59**, 2853.
20 P. Cassoux, R. Dartiguepeyron, C. David, D. de Montauzon, J.-B. Tommasino and P.-L. Fabre, *Actual. Chim.*, 1994, 49 and references therein.
21 Stoe, IPDS Manual, version 2.87, Stoe & Cie, Darmstadt, Germany, 1997.
22 SIR-97, Program for Crystal Structure Solution. A. Altomare, M. C. Burla, M. Camalli, G. L. Cascarano, C. Giacovazzo, A. Guagliardi, A. G. G. Moliterni, G. Polidori and R. Spagna, *J. Appl. Crystallogr.*, 1999, **32**, 115.
23 G. M. Sheldrick, SHELXL-97, Program for the Refinement of Crystal Structures from Diffraction Data, Institüt für Anorganische Chemie der Universität, Tammanstrasse 4, D-3400 Göttingen, Germany, 1998.
24 D. T. Cromer and J. T. Waber, *International Tables for X-Ray Crystallography*, vol. IV, Kynoch Press, Birmingham, England, 1974.
25 R. J. Letcher, W. Zhang, C. Bensimon and R. J. Crutchley, *Inorg. Chim. Acta*, 1993, **210**, 183.
26 (*a*) E. W. Ainscough, E. N. Baker, M. L. Brader, A. M. Brodie, S. L. Ingham, J. M. Waters, J. V. Hanna and P. C. Healy, *J. Chem. Soc., Dalton Trans.*, 1991, 1243; (*b*) R. J. Crutchley, K. McCaw, F. L. Lee and E. J. Gabe, *Inorg. Chem.*, 1990, **29**, 2576; (*c*) R. J. Crutchley, R. Hynes and E. J. Gabe, *Inorg. Chem.*, 1990, **29**, 4921.
27 M. L. Brader, E. W. Ainscough, E. N. Baker and A. M. Brodie, *Polyhedron*, 1989, **8**, 2219.
28 M. H. Chisholm, K. Folting, J. C. Huffman and N. S. Marchant, *Polyhedron*, 1984, **3**, 1033.
29 B. Lunelli, S. Roffia, C. Paradisi and G. F. Pedulli, *J. Chem. Soc., Faraday Trans.*, 1994, **90**, 137.
30 (*a*) L. R. Nassimbeni and A. L. Rodgers, *Acta Crystallogr., Sect. B*, 1976, **32**, 257; (*b*) J. A. C. van Ooijen, J. Reedijk and A. L. Speck, *Inorg. Chem.*, 1979, **18**, 1184.
31 M. L. Calatayud, I. Castro, J. Sletten, J. Cano, F. Lloret, J. Faus, M. Julve, G. Seitz and K. Mann, *Inorg. Chem.*, 1996, **35**, 2858.
32 H. G. Khorama, *Chem. Rev.*, 1953, **53**, 145.
33 F. Kurzer and K. Douragui-Zadeh, *Chem. Rev.*, 1967, **67**, 107.
34 R. J. Crutchley and M. L. Naklicki, *Inorg. Chem.*, 1989, **28**, 1955.
35 P.-L. Fabre, C. Pena, A. M. Galibert, B. Soula, G. Bernardinelli, B. Donnadieu and P. Castan, *Can. J. Chem.*, 2000, **78**, 280.
36 M. Ito and R. West, *J. Am. Chem. Soc.*, 1963, **85**, 2580.
37 K. Kohler, W. Massa, G. Offermann, G. Seitz and R. Sutrisno, *Chem. Ber.*, 1985, **118**, 1903.
38 F. E. Mabbs and D. J. Machin, *Magnetism and Transition Metal Complexes*, Chapman and Hall Ltd., London, 1973.
39 G. A. van Albada, J. J. A. Kolnaar, W. J. J. Smeets, A. L. Spek and J. Reedijk, *Eur. J. Inorg. Chem.*, 1998, 1337.
40 L. Driessen, R. M. de Vos, A. Etz and J. Reedijk, *Inorg. Chim. Acta*, 1995, **235**, 2884.
41 R. Cortes, J. I. Ruiz de Larramendi, L. Lezama, T. Rojo, K. Urtiaga and M. I. Arriortua, *J. Chem. Soc., Dalton Trans.*, 1992, 2723.
42 S. R. Batten, B. F. Hosskins, B. Moubaraki, K. S. Murray and R. Robson, *J. Chem. Soc., Dalton Trans.*, 1999, 2977.
43 (*a*) A. Meyer, A. Gleizes, J. J. Girerd, M. Verdaguer and O. Kahn, *Inorg. Chem.*, 1982, **21**, 1729; (*b*) L. Sacconi, F. Mani and A. Bencini, *Compr. Coord. Chem.*, 1987, **5**, 1.
44 Simulated Voltammograms (ESP) have been computed with Nervi's program. Copyright by Carlo Nervi. This package can be downloaded at the Internet address: http://lem.ch.unito.it/chemistry/esp_manual.html.
45 D. T. Pierce and W. E. Geiger, *J. Am. Chem. Soc.*, 1989, **111**, 7636.
46 B. Carré, J. Paris, P.-L. Fabre, S. Jourdannaud, P. Castan, D. Deguenon and S. Wimmer, *Bull. Soc. Chim. Fr.*, 1990, **127**, 367.
47 B. Trémillon, *Electrochimie Analytique et Réactions en Solution*, Masson, Paris, 1993, ch. X.
48 F. Dumestre, B. Soula, A. M. Galibert, P.-L. Fabre, G. Bernardinelli, B. Donnadieu and P. Castan, *J. Chem. Soc., Dalton Trans.*, 1998, 4131.
49 B. Soula, A. M. Galibert, B. Donnadieu and P.-L. Fabre, *Inorg. Chim. Acta*, 2001, **324**, 90.
50 A. E. Kaifer and M. Gómez-Kaifer, *Supramolecular Electrochemistry*, Wiley-VCH, Weinheim, 1999.